

# Thermal Strain of High Strength Polyethylene Fiber in Low Temperature

Atsuhiko Yamanaka,<sup>1</sup> Tooru Kitagawa,<sup>2</sup> Masayuki Tsutsumi,<sup>3</sup> Toshihiro Kashima,<sup>4</sup> Hiroyuki Fujishiro,<sup>5</sup> Kimiko Ema,<sup>6</sup> Yoshinobu Izumi,<sup>6</sup> Shigehiro Nishijima<sup>6</sup>

<sup>1</sup>Advanced Textiles R & D Center, Research Center, Toyobo Co., Ltd., 2-1-1, Katata, Ohtsu, Shiga 520-0292, Japan

<sup>2</sup>Analytical Research Center, Toyobo Research Center, Toyobo Co., Ltd., 2-1-1, Katata, Ohtsu, Shiga 520-0292, Japan

<sup>3</sup>Film Laboratory, Advanced Materials Research Department, TOYOBO Research Center, CO., LTD., Address : 2-1-1, Katata, Ohtsu, Shiga 520-0292, Japan

<sup>4</sup>Hamamatsu Technopolis, Shizuoka University, Hamamatsu, Shizuoka 431-3215, Japan

<sup>5</sup>Department of Materials Science and Technology, Faculty of Engineering, Iwate University, Ueda 4-3-5, Morioka 020-8551, Japan

<sup>6</sup>Department of Nuclear Engineering, Graduate School of Engineering, Osaka University, Yamadaoka 2-1, Suita, Osaka 565-0871, Japan

Received 19 September 2003; accepted 8 April 2004

DOI 10.1002/app.20890

Published online 16 July 2004 in Wiley InterScience (www.interscience.wiley.com).

**ABSTRACT:** High strength polyethylene fiber (Toyobo, Dyneema® fiber: hereinafter abbreviated to DF) has a negative thermal expansion coefficient. Relation between fiber structure and thermal strain of DF used as reinforcement of DF reinforced plastic (DFRP) for cryogenic use was investigated. The crystallinities and orientation angles of several kinds of polyethylene fibers having different modulus from 15 to 134Gpa (herein after abbreviated to DFs) were measured by NMR and X-ray. We obtained the parameters of the mechanical series-parallel model composed of crystal and amorphous by crystallinity and modulus. Thermal expansion coefficients of DFs were estimated by mechanical series-parallel model. All DFs having different modulus showed negative thermal expansion coefficients in the temperature

range from 180 to 300K, and absolute values of those markedly increased by increasing tensile modulus of DF. The estimated thermal expansion coefficients showed negative values, and thermal strains showed a similar curve to observed ones mostly. Average thermal expansion coefficients in the temperature range from 180 to 300K estimated by mechanical model agreed with the observed ones. © 2004 Wiley Periodicals, Inc. *J Appl Polym Sci* 93: 2918–2925, 2004

**Key words:** negative thermal expansion; polyethylene fiber; low temperature

## INTRODUCTION

High strength polyethylene fiber (Toyobo, Dyneema®, DF, Osaka, Japan) has a negative thermal expansion coefficient.<sup>1,2</sup> Using this unique property, DF reinforced plastics (DFRPs) have been developed in the cryogenic field as coil bobbins<sup>3</sup> or spacers<sup>4</sup> for superconducting coil and in the optical field as package of fiber Bragg grating for optical filter.<sup>5</sup> It is known that wire motions wound on superconducting coil bobbin composed of DFRP are contracted and the superconducting coil becomes more stable.<sup>6,7</sup> The stability of the superconducting coil is guessed to be caused by negative thermal expansion.<sup>3,6–10</sup> Temperature dependence of optical property of fiber Bragg grating can be controlled by using a package composed of DFRP.<sup>5</sup> The negative expansion property is important for applications for cryogenic or information use as low frictional property,<sup>11,12</sup> high thermal conductivity,<sup>13,14</sup> and high electrical resistance.<sup>15</sup>

It is known from X-ray studies that the thermal expansion coefficient of polymer crystals, for example polyethylene, in the direction of the chain axis measured is negative for most if not all polymers.<sup>16,17</sup> The thermal vibration perpendicular to the polymer chain contributes to the negative thermal expansion in the chain axis. The negative thermal expansion is explained by the "Linear Chain Model."<sup>18–20</sup> So, highly oriented and highly crystallized polyethylene is expected to show a negative thermal expansion in the oriented direction by treating as a composite consisting of a crystal part showing negative thermal expansion and an amorphous part showing positive thermal expansion.<sup>21,22</sup>

In this work, the relation between fiber structure and thermal strain of DF used as reinforcement of DFRP for cryogenic use was investigated. The crystallinities and orientation angles of several kinds of polyethylene fibers having different modulus from 15 to 134Gpa (herein after abbreviated to DFs) were measured by NMR and X-ray. Initially, the relation between crystallinity and thermal expansion coefficients

Correspondence to: A. Yamanaka (Atsuhiko Yamanaka@kt.toyobo.co.jp).

of DFs were investigated. And we obtained the parameters of the series-parallel model composed of crystal and amorphous by crystallinity and modulus. Thermal expansion coefficients of DFs were estimated by the mechanical series-parallel model to inspect applicability of the mechanical model to thermal expansion of DF.

## EXPERIMENTAL

### Sample

Four kinds of DFs (Dyneema®, DF(A–D)) having different modulus were used. Tensile modulus of DFs are as follows: DF(A): 15GPa; DF(B): 51GPa; DF(C): 85GPa; and DF(D): 134GPa.

### Measurements

#### Thermal expansion coefficient

Thermal expansion coefficients were measured on DFs by thermomechanical analysis (TMA) on tensile mode. TMA measurements were carried out on a MAC Science TMA 4000S. Samples were run in TMA between 153 and 413 K at scanning rate of 10 deg/min. Sample length was 15 mm. The loading was 500 g/mm<sup>2</sup>.

#### Crystallinity and orientation angle

Negative thermal expansivity of DF in fiber direction is guessed to be caused by contribution of chain axis of crystalline regions, so we investigated the crystallinities and orientation angles of crystals to fiber axis of the DFs. Crystallinities of DFs were measured by solid state high resolution NMR. Orientation angles of DFs were measured by X-ray diffraction.

It is known that crystal and amorphous have different chemical shifts in solid state <sup>13</sup>C-NMR spectra of polyethylene.<sup>23–27</sup> And it is also known about polyethylene that relaxation times of solid state NMR are different between crystal and amorphous because of difference of molecular motions.<sup>26–28</sup> So, a lot of studies by solid state NMR were reported using peak separation by difference of chemical shifts<sup>23–27</sup> or analysis of relaxation times by difference of molecular motions<sup>26–28</sup> to investigate phase structure of polyethylene. In this work, solid state high resolution NMR spectra of DFs were measured for peak separation to estimate the crystallinities of DFs. Solid state NMR measurements were carried out on a Varian XL-300 (<sup>13</sup>C, 75.5MHz). NMR spectra were measured by Cross-Polarization (CP) high power proton decoupling (DD) magic angle spinning (MAS) method. Pulse width was 5 μs, dipole DD power was 50 kHz, and MAS rate was 3.5kHz.

Orientation angle of crystalline phase in DFs was estimated by intensity distribution of X-ray diffraction

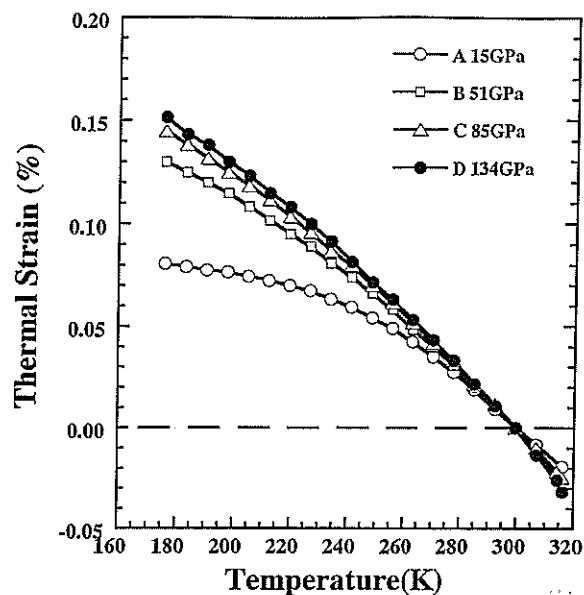


Figure 1 Thermal strain of DF(A–D) in fiber direction.

spot. Rigaku RU – 200 (40 kV x 100 mA) was used with X-ray diffraction on Ni-filtered CuK $\alpha$  ( $\lambda = 0.1548$  nm). (200) diffraction spot was used for estimating orientation angles.

## RESULTS AND DISCUSSION

### Thermal strain of DFs

Thermal strains of DFs in fiber direction measured by TMA are shown in Figure 1. All DFs expand by cooling down (negative thermal expansion). Negative thermal expansion coefficient increases with increasing tensile modulus of DF. Temperature dependence becomes slower by cooling down.

The negative thermal expansion coefficients of DFs are inferred to be caused by the thermal strain of the crystal phase in chain axis. So, to investigate the relation between negative thermal expansion and fiber structure of DF, solid state high resolution NMR were measured for analysis of crystallinity, and X-ray diffraction measurements were carried out for estimating the orientation angles of DFs. We report those in the following section.

### Crystallinity of DFs

<sup>13</sup>C-CP-MAS solid state high resolution NMR spectra of DF(A–D) are shown in Figure 2. In the spectra of DF(A), a main peak is observed at 33ppm. It is a sharp peak due to orthorhombic crystal (ORC).<sup>23–27</sup> The broad shoulder is observed at the higher field side of the ORC signal. The shoulder peak at 31ppm is due to amorphous region (noncrystal: NC).<sup>23–27</sup> The other broad shoulder is observed at the lower field side of

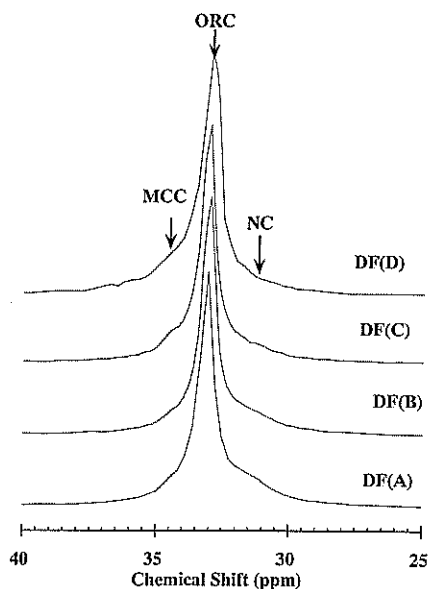


Figure 2  $^{13}\text{C}$  CP-MAS solid state high resolution NMR spectra of DF(A-D).

the ORC signal. The shoulder at 34ppm is due to monoclinic crystal (MCC).<sup>23-27</sup> Comparing DF(A) with DF(B-D), the 31ppm broad shoulder is small as in higher modulus DF. It suggests that crystallinity increases and amorphous decreases as in higher modulus DF. On the contrary, the 34ppm peak due to MCC increases as in higher modulus DF. This result agrees with the NMR studies by A. Kaji et al.<sup>26,27</sup> The increase of MCC phase is reported to be caused by drawing.<sup>26,27,29</sup> The structure of MCC is similar to that of ORC in polyethylene.<sup>29</sup>

The analysis of crystal regions and amorphous is possible by peak separation to the two components: crystal (ORC (33ppm), MCC (34ppm)) and amorphous (NC, 31ppm). Separation of  $^{13}\text{C}$ -CP-MAS solid state NMR spectra of DF(A) by some Lorentzians is shown in Figure 3. Intermediate regions between crystal and amorphous were studied by NMR, but in this work, we don't discuss the intermediate phase.<sup>26,27</sup> For simplification, we discuss the fiber structure by only the two components: crystal (ORC, MCC) and NC. In the case of other DFs (DF(B, C, and D)), NMR spectra are separated by three peak components as DF(A). Crystallinities and components of ORC and MCC estimated by peak separation of DF(A-D) are shown in Figure 4. It is shown that crystallinity is higher in DFs of higher modulus, especially the degree of crystallinity in DF(D), which is estimated at nearly 100%.

#### Orientation angle

An X-ray diffraction photograph of DF(A) is shown in Figure 5. The orientation angle of crystals was esti-

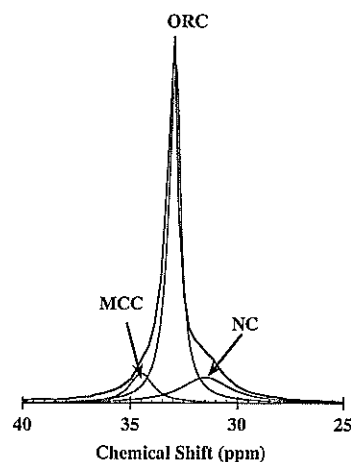


Figure 3 Separation of  $^{13}\text{C}$  CP-MAS solid state high resolution NMR spectra of DF(A) by some Lorentzians.

ated by azimuthal intensity distribution of the (200) diffraction according to the following equation.<sup>30</sup>

$$\langle \sin^2 \phi \rangle = \int I(\phi) \sin^3 \phi d\phi / \int I(\phi) \sin \phi d\phi \quad (1)$$

where  $\phi$  is the azimuthal angle to the fiber axis, and  $I(\phi)$  the intensity distribution of the (200) diffraction along the azimuthal direction. Orientation angles of DF(B-D) were estimated by similar analysis. Estimated orientation angles of DF(A-D) are shown in Figure 6. The orientation angle is smaller, and tensile modulus is higher. So, highly oriented DF has a high modulus. But every DF has a small orientation angle.

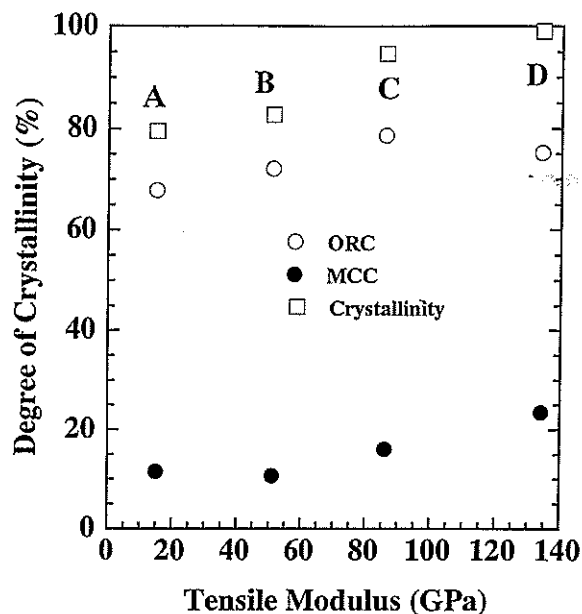


Figure 4 Crystallinity and tensile modulus of DF(A-D).

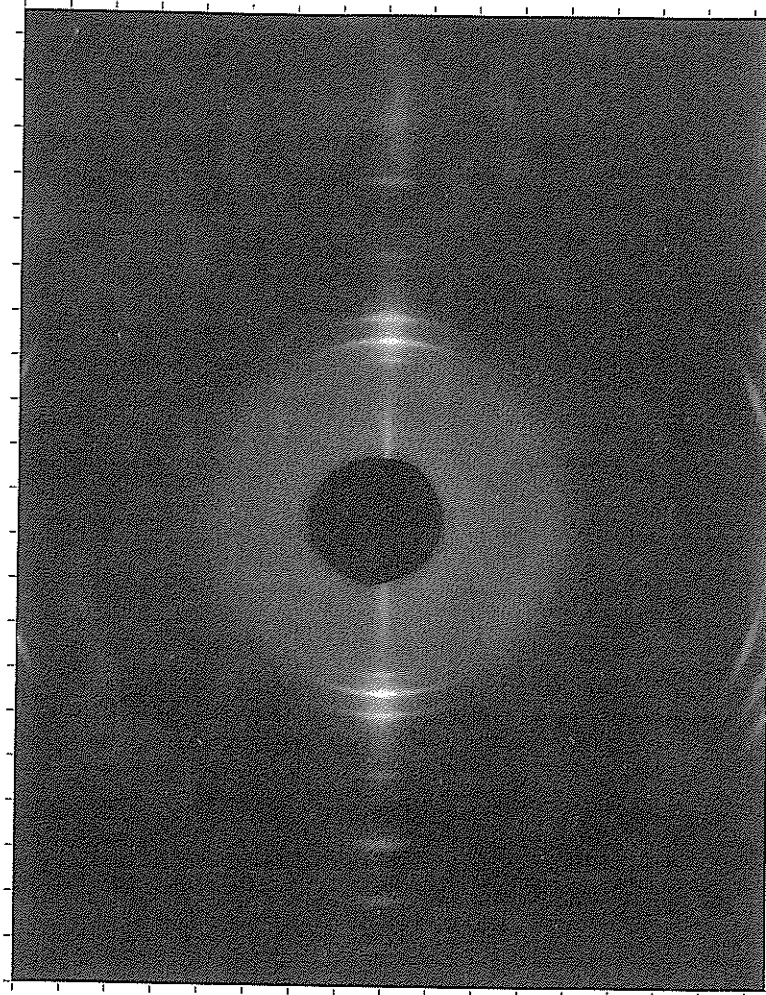


Figure 5 X-ray diffraction photograph of DF(A).

So the DFs are considered as nearly perfect oriented fiber, and the chain axis in the crystal region are considered as fiber axis in the following sections.

#### Dependence of thermal expansion coefficient on crystallinity of DF

In the first sections, crystallinities and orientation angles in crystal of DFs were estimated by NMR and X-ray measurement. And we considered the chain axis in crystal as fiber axis. So, we need not consider the influence of the orientation angle. Crystalline of polyethylene shows negative thermal expansion along the chain axis, so negative thermal expansion is expected to increase with increasing crystallinity. In this section, the relation between crystallinity and thermal expansion is investigated. Dependence of average thermal expansion coefficients in the temperature range from 300 to 180 K on the crystallinity is shown in Figure 7. Negative thermal expansion increases with increasing crystallinity. This suggests a contribution of the crystal region to negative thermal expansion of DF. But ther-

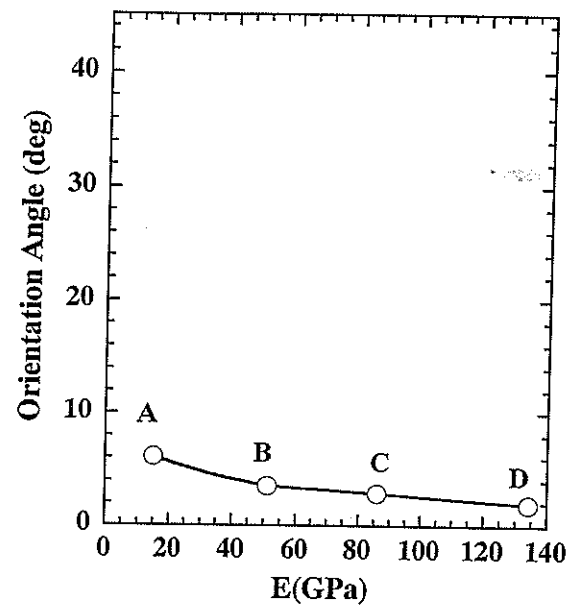


Figure 6 Orientation angles and tensile modulus of DF(A-D).

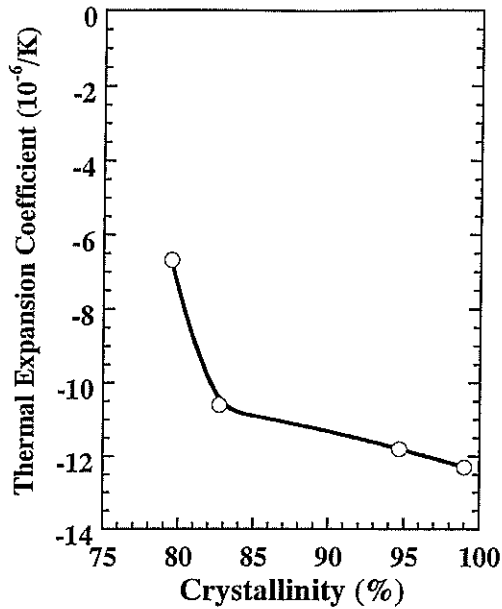


Figure 7 Relation of crystallinities and average thermal expansion coefficients in temperature range of 180–300K of DF(A–D).

mal expansion coefficients between DF(A) and DF(B) are much different in spite of a small difference of crystallinity. Crystallinity of DF(A) is 79% and that of DF(B) is 81%. So the increasing negative thermal expansion cannot be explained only by crystallinity of DFs. In the following sections, the mechanical series-parallel model is applied to DFs for thermal strain.

#### Parameters of mechanical series-parallel model

To understand the negative thermal expansion of DFs, mechanical series-parallel model composed of crystal region and amorphous region was introduced here. In

this mechanical model, chain axis in the crystal region is extended and aligned to fiber axis, because orientation angles are nearly 0 as shown in Figure 8. The estimation of  $x_{IIa}$ ,  $x_{IIc}$ ,  $y_I$ , and  $y_{II}$  in Figure 8 is necessary for completion of the mechanical series-parallel model. The parameters  $x_{IIa}$  and  $y_{II}$  were estimated by Young's modulus and crystallinity as follows. In the estimation, chain axis of crystal is treated as aligned to fiber axis.

The parameters of the mechanical model are defined as follows:  $E_I$ , tensile modulus of part I, which is continuous crystal;  $E_{II}$ , tensile modulus of part II, composed of crystal and amorphous by series combination;  $E_c$ , tensile modulus of crystal in chain direction;  $E_a$ , tensile modulus of amorphous;  $x$ , length of amorphous part;  $y$ , width of part II;  $v_a = x_{IIa}y_{II}$ , volume fraction of amorphous.

Those definitions are shown in Figure 8. Total tensile modulus ( $E$ ) of DF are shown in the following formula:

$$E = [y_I E_I + y_{II} E_{II}] \quad (2)$$

$E_I$  and  $E_{II}$  are shown in the following formulas (3) and (4):

$$E_I = E_c \quad (3)$$

$$E_{II} = E_c E_a / [x_{IIc} E_a + x_{IIa} E_c] \quad (4)$$

$$x_{IIc} + x_{IIa} = 1, y_I + y_{II} = 1 \quad (5)$$

$E$  of DFs are experimental values.  $E_c$  is 235GPa obtained by Nakamae et al.<sup>31</sup> and  $E_a$  is 0.3GPa obtained by Chen et al.<sup>19</sup> The volume fraction of amorphous  $v_a = x_{IIa}y_{II}$  are estimated by solid state NMR measurements as mentioned above. The parameters of me-

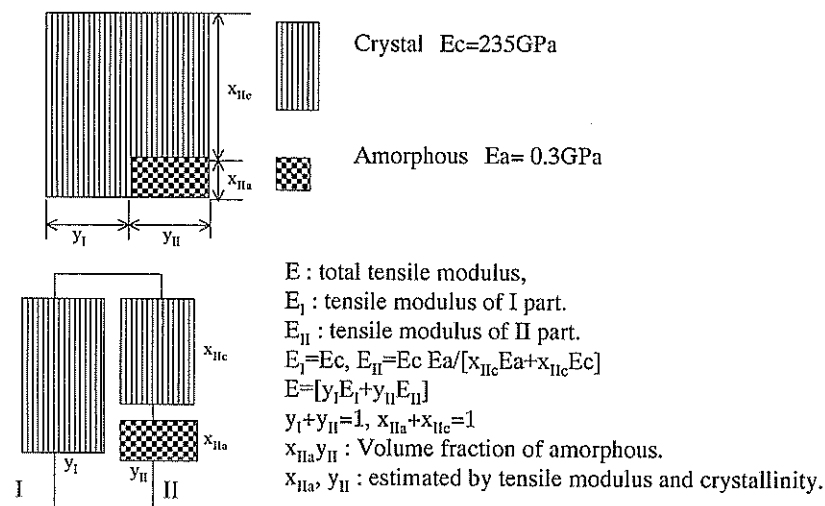
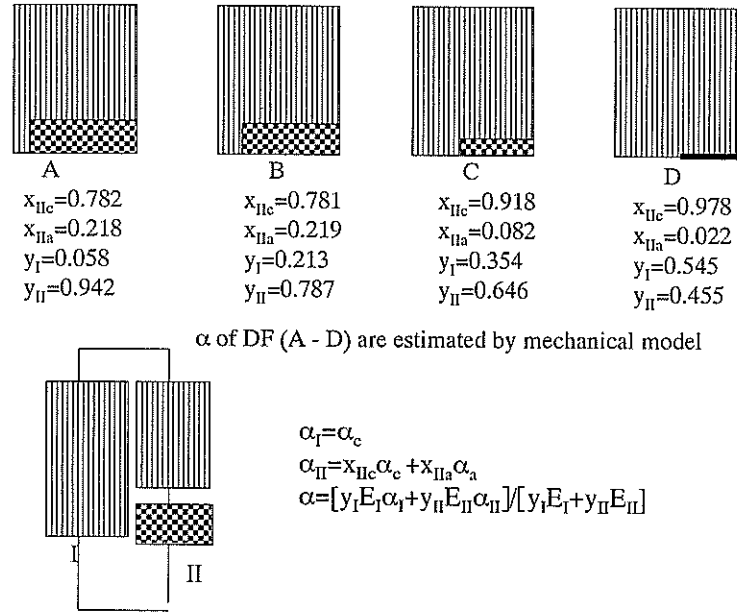


Figure 8 Schematic diagram showing the structure of DF by mechanical series-parallel model.



**Figure 9** Schematic diagram of DF(A-D) by mechanical series-parallel model estimated by crystallinities, orientation angles, and tensile modulus.

chanical model ( $x_{IIc}$ ,  $x_{IIa}$ ,  $y_I$ , and  $y_{II}$ ) can be estimated by the substitution of the numerical values above-mentioned into the eqs. (2)–(5).

The obtained  $x_{IIc}$ ,  $x_{IIa}$ ,  $y_I$ , and  $y_{II}$  are shown in Figure 9 and Table I. DF(A) is composed of part II for the most part and is similar to the series model. On the other hand, part I increases in DF(B, C, and D) more than in DF(A).

**Estimation of the thermal expansion coefficients of DF by mechanical series-parallel model**

Thermal expansion coefficients of DF are estimated by the mechanical series-parallel model here by the following formulas:

$$\alpha_I = \alpha_c \tag{6}$$

$$\alpha_{II} = x_{IIc}\alpha_c + x_{IIa}\alpha_a \tag{7}$$

$$\alpha = [y_I E_I \alpha_I + y_{II} E_{II} \alpha_{II}] / [y_I E_I + y_{II} E_{II}] \tag{8}$$

**TABLE I**  
Parameter of DF(A-D) in the Mechanical Model

	E (GPa)	Crystallinity (%)	$x_{IIc}$	$x_{IIa}$	$y_I$	$y_{II}$
DF(A)	15	79.5	0.782	0.218	0.058	0.942
DF(B)	51	82.7	0.781	0.219	0.213	0.787
DF(C)	85	94.7	0.918	0.082	0.354	0.646
DF(D)	134	99.0	0.978	0.022	0.544	0.455

In eqs. (6)–(8) the thermal expansion parameters are defined as follows:  $\alpha$ , thermal expansion coefficient of DF;  $\alpha_I$ , thermal expansion coefficient of part I;  $\alpha_{II}$ , thermal expansion coefficient of part II;  $\alpha_c$ , thermal expansion coefficient of crystal part in chain axis; and  $\alpha_a$ , thermal expansion coefficient of amorphous region.

Calculated values by the Linear Chain Model with consideration for temperature dependence by Choy et al.<sup>20</sup> are used as numerical values of  $\alpha_c$ . It is known that calculated  $\alpha_c$  by the Linear Chain Model shows negative values and that absolute value decreases by cooling down.<sup>20</sup> This behavior is known to agree with experimental results.<sup>20</sup>

Tensile modulus of the crystal region in chain direction  $E_c$  is assumed as 235GPa reported as the experimental value.<sup>31</sup> And temperature independence of  $E_c$  is reported.<sup>31</sup> On the other hand, estimations of temperature dependence of  $E_c$  by calculation are reported.<sup>32–35</sup> To clear the temperature dependence of  $E_c$ , more detailed discussion will be necessary. The change of  $E_c$  reported is 4 ~ 60GPa by cooling from 300K to 4K.

On the other hand, it is known that the thermal expansion coefficient of amorphous region  $\alpha_a$  shows positive values and that the absolute value is larger than those of crystal in chain direction  $\alpha_c$ .<sup>20</sup> Tensile modulus of amorphous region  $E_a$  increases by cooling down.<sup>20</sup> The values reported by Choy et al.<sup>20</sup> are used as  $\alpha_a$  and  $E_a$ .

The temperature dependence of thermal expansion coefficients of DF(A-D) are estimated by putting the

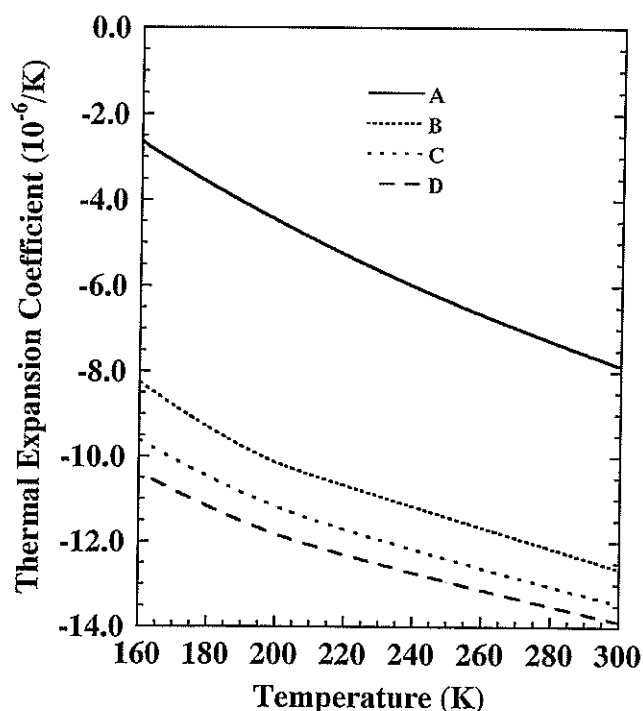


Figure 10 Thermal expansion coefficients of DF(A-D) estimated by mechanical model.

values above-mentioned into eqs. (6)–(8). The calculated results are shown in Figure 10. It is shown that all DFs show negative thermal expansion coefficients. The absolute value of the negative thermal expansion coefficients of DF(D) is the largest in all of the DFs and it decreases in order of C, B, A. Those absolute values decrease by cooling down because of decreasing the absolute value of negative expansion in the crystal region along the chain axis.

#### Comparison of thermal strain of DFs between observed and calculated values

The thermal strains of DFs are estimated by the temperature dependence of thermal expansion coefficients in the first section. Those are compared with observed values in Figure 11. In the case of DF(A), the observed curve shows similar behavior to the calculated one, even if the observed strain is larger than the calculated one in the temperature range about 200 ~ 250K. Calculated curves of DF(B, C, and D) have good agreement with observed ones. Average thermal expansion coefficients in the temperature range from 180 to 300K are compared in Figure 12. Calculated thermal expansion coefficients of DFs agree with observed ones mostly. So, average thermal expansion coefficients of DF(A-D) in the temperature range from 180 to 300K are explained by the mechanical series-parallel model.

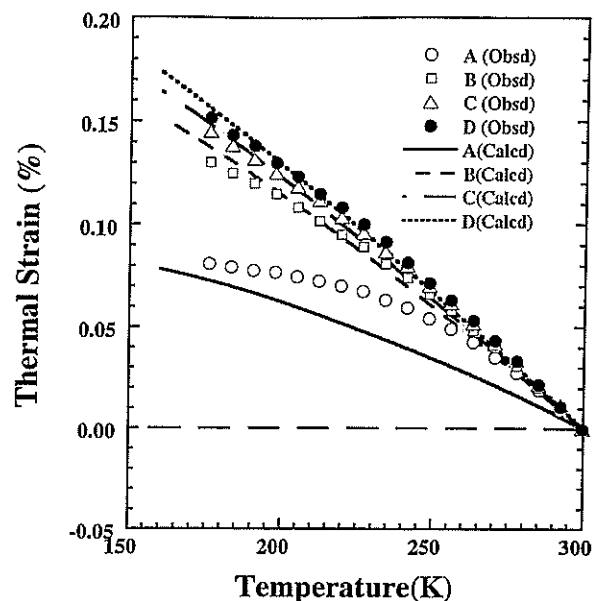


Figure 11 Thermal strain of DF(A-D) in fiber direction. Markings represent the observed values, and the lines are calculated.

Comparing among DF(A-D) in Figures 9 and 12 and Table I, crystallinity of DF(A) and DF(B) are not so different, but negative thermal expansion are much different. It is guessed to be caused by increasing part I shown in Figure 9 from A to B. Part I of DF(B) is about 4 times larger than that of DF(A). So, in the case

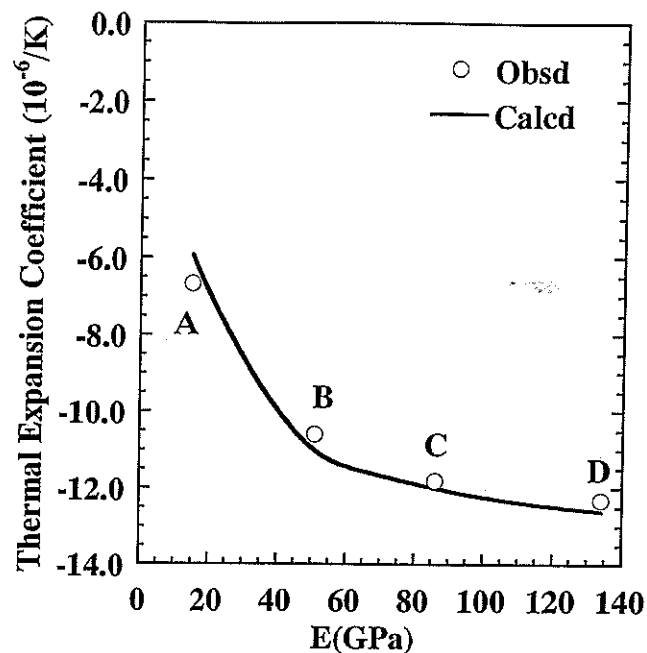


Figure 12 Average thermal expansion coefficients of DF(A-D) in the temperature range of 180–300 K. Markings represent the observed values, and the line is calculated.

of same crystallinity, negative thermal expansion can increase by increasing part I in the mechanical model.

With the above, negative thermal expansion of DF(A-D) is explained by the mechanical series-parallel model composed of crystal and amorphous.

### CONCLUSION

Thermal strain and crystallinity were measured for several kinds of high strength polyethylene fiber (DF(A-D)) having different modulus, which were 15-134GPa. The following conclusions were drawn:

1. All DFs showed negative thermal expansion coefficients in the temperature range from 180 to 300K, and absolute values of those markedly increased by increasing the tensile modulus of DF.
2. The degree of crystallinities of DFs were 80 ~ 99%, and negative thermal expansion of DF increased with increasing crystallinity and tensile modulus.
3. The mechanical series-parallel model composed of crystal and amorphous was applied to DFs by using tensile modulus and crystallinity. Thermal expansion coefficients of DFs were estimated by the mechanical model. The estimated thermal expansion coefficients showed negative values, and thermal strains mostly showed a curve similar to observed ones.
4. Average thermal expansion coefficients in the temperature range from 180 to 300K estimated by the mechanical model agreed with observed ones.

With the above-mentioned, the mechanical series-parallel model composed of crystal and amorphous could be applied to DFs for negative thermal expansion coefficients.

The authors thank Dr. Yasuo Ohta and Dr. Tadao Kuroki of Toyobo Co., Ltd. for preparing DF samples. The authors also thank professor Dr. Manabu Ikebe of Iwate University, Dr. Masao Murano of Saga University, and Dr. Atsushi Kaji of Toyobo Co., Ltd. for their encouragement. Thanks also are due to the experimental assistant group of Polymer Institute in Toyobo Co., Ltd. for experimental assistance, and to the Dyneema Department of Toyobo Co., Ltd. for encouragement.

### REFERENCES

1. Scholle, K. F. M. J. 9th Int. SAMPE, European Chapter, Milano, Italy, June 14-16, 1988.
2. Kashima, T.; Yamanaka, A.; Takasugi, S.; Nishihara, S. *Adv Cryog Eng* 2000, 46, 329.
3. Kashima, T.; Yamanaka, A.; Yoneda, E. S.; Nishijima, S.; Okada, T. *Adv Cryog Eng* 1996, 41, 441.
4. Yamanaka, A.; Kashima, T.; Nishijima, S.; Okada, T. *Cryog Eng* 1997, 32, 330.
5. Oe, K.; Hashimoto, T.; Yano, H.; Mikami, O.; Kakinuma, A.; Yamanaka, A. *Proc of ECOC* 2002.
6. Yamanaka, A.; Kashima, T.; Hosoyama, K. *IEEE Trans Appl Supercond* 2001, 11, 4061.
7. Yamanaka, A.; Kashima, T.; Hosoyama, K.; Nago, S.; Takao, T.; Sato, S.; Takeo, M. *Physica-C* 2002, 377.
8. Kamijo, H.; Nemoto, K.; Kashima, T. *Meeting on Cryogenics and Superconductivity* 1993, 105.
9. Takao, T.; Watanabe, K.; Moriya, T.; Kubosaka, T.; Kashima, T.; Yamanaka, A.; Fukui, S. *Proc. of MT* 1998, 15.
10. Takeda, K.; Chiba, M.; Fukuda, K.; Sakagami, Y.; Shibuya, M.; Miyashita, K.; Moriai, H.; Kamata, K. *Proc of ICEC* 1999, 17.
11. Iwabuti, A.; Arai, H.; Yoshino, Y.; Sugimoto, M.; Yoshida, K.; Kashima, T.; Inui, H. *Cryogenics* 1995, 35, 35.
12. Takao, T.; Nemoto, T.; Konda, H.; Kashima, T.; Yamanaka, A. *Proc of ICEC16/ICMC* 1993, 1997.
13. Fujishiro, H.; Ikebe, M.; Kashima, T.; Yamanaka, A. *Jpn J Appl Phys* 1997, 36, 5633.
14. Fujishiro, H.; Ikebe, M.; Kashima, T.; Yamanaka, A. *Jpn J Appl Phys* 1998, 37, 1994.
15. Nitta, T.; Chiba, M.; Kashima, T.; Takao, T. *Proc 15<sup>th</sup> Int Conf Magnet Technology* Oct. 1997, 1159.
16. Kobayashi, Y.; Keller, A. *Polymer* 1970, 11, 114.
17. Davis, G. T.; Eby, R.; Coloson, J. P. *J Appl Phys* 1970, 41, 4316.
18. Chen, F. C.; Choy, C. L.; Young, K. *J Polym Sci* 1980, 18, 2313.
19. Chen, F. C.; Choy, C. L.; Young, K.; Wong, S. *J Polym Sci* 1981, 19, 971.
20. Choy, C. L.; Wong, S. P.; Young, K. *J Polym Sci* 1984, 22, 979.
21. Perico, A.; Cuniberti, C. *J Polym Sci* 1977, 15, 1435.
22. Choy, C. L.; Chen, F. C.; Ong, E. L. *Polymer* 1979, 20, 1191.
23. VanderHart, D. L.; Khoury, F. *Polymer* 1984, 25, 1589.
24. Yamanobe, T.; Sorita, T.; Komoto, T.; Ando, I.; Sato, H. *J Mol Structure* 1985, 131, 267.
25. Kitamaru, R.; Horii, F.; Murayama, M. *Macromolecules* 1986, 19, 636.
26. Kaji, A.; Ohta, Y.; Yasuda, H.; Murano, M. *Polym J* 1990, 22, 455.
27. Kaji, A.; Yamanaka, A.; Murano, M. *Polym J* 1990, 22, 893.
28. Horii, F.; Kitamaru, R.; Maeda, S.; Saika, A.; Terao, T. *Polym Bull* 1985, 13, 179.
29. Seto, T.; Hara, T.; Tanaka, K. *Jpn J Appl Phys* 7, 1968, 1, 31.
30. Kitagawa, T.; Murase, H.; Yabuki, K. *J Polym Sci, Part B: Polym. Phys* 1998, 36, 39.
31. Nakamae, K.; Nishino, T.; Ohkubo, H. *J Macromol Sci Phys*, B 1991, 30, 1.
32. Shimanouchi, T.; Asahina, M.; Enomoto, S. *J Polym Sci* 1962, 59, 93.
33. Tashiro, K.; Kobayashi, M.; Tadokoro, H. *Macromolecules* 1977, 10, 731.
34. Karasawa, N.; Dasgupta, S.; Goddard III, W. A. *J Phys Chem* 1991, 95, 2260.
35. Tashiro, K. *Polymer Preprint* 1999, 3867.